

## Dimensional crossover in the magnetic properties of highly anisotropic antiferromagnets. II. Paramagnetic phase

N. Majlis and S. Selzer

*Scuola Normale Superiore, I-56100 Pisa, Italy*

*and Instituto de Física, Universidade Federal Fluminense, Outeiro de São Joao Batista S/N, 24020 Niterói, Rio de Janeiro, Brazil*

G. C. Strinati

*Dipartimento di Fisica, Università di Roma La Sapienza, I-00185 Rome, Italy*

(Received 25 September 1992)

We calculate the magnetic properties of a spin- $\frac{1}{2}$  antiferromagnet, described by a Heisenberg model with anisotropic exchange coupling, for the high-temperature (paramagnetic) phase by extending our previous calculations for the low-temperature (broken-symmetry) phase based on random-phase-approximation (RPA) and modified RPA decouplings within the Green's-function method. We find again that the dimensional crossover from three to two dimensions occurs at  $\epsilon \approx 10^{-3}$ , where  $\epsilon = J_{\perp}/J_{\parallel}$  is the anisotropy ratio between the interplane and intraplane exchange couplings. We obtain the coherence length for spin-deviation correlations as a function of temperature and  $\epsilon$ , and compare our results with other theoretical treatments for the two-dimensional ( $\epsilon=0$ ) limit. We find good agreement between our calculation and neutron data on  $\text{La}_2\text{CuO}_{4-y}$  compounds when  $\epsilon \sim 10^{-4}-10^{-6}$ .

### I. INTRODUCTION

The magnetic properties of highly anisotropic magnetic systems have lately become of particular interest, owing to the layered structures present in the magnetic parent compounds of the high-temperature superconducting perovskites. In particular,  $\text{La}_2\text{CuO}_4$  and  $\text{YBa}_2\text{Cu}_3\text{O}_6$  have a fairly large Néel temperature (of several hundred K) and show antiferromagnetic correlations which are strongly anisotropic.<sup>1</sup> Current estimates of the effective exchange coupling  $J_{\parallel}$  within the  $\text{CuO}_2$  planes yield an unusually large value ( $J_{\parallel} \sim 0.1$  eV), while the interplane coupling  $J_{\perp}$  is expected to be quite small. In particular, for  $\text{La}_2\text{CuO}_4$  the anisotropy ratio  $\epsilon = J_{\perp}/J_{\parallel}$  is estimated to range from  $10^{-4}$  to  $10^{-5}$  (Ref. 1) while for  $\text{YBa}_2\text{Cu}_3\text{O}_6$ ,  $\epsilon \sim 10^{-2}-10^{-3}$  is somewhat larger (Ref. 2). Neutron-scattering experiments<sup>1</sup> in  $\text{La}_2\text{CuO}_4$  were further interpreted in terms of an intraplane correlation length  $\xi_c$  that remains quite large up to temperatures of the order  $1.5T_N$  (with the Néel temperature  $T_N \sim 200$  K).

The discovery of the *quasi-two-dimensional* behavior of these magnetic systems has prompted an extensive theoretical work on the *two-dimensional* quantum Heisenberg antiferromagnet, including renormalization-group treatments of the nonlinear  $\sigma$  model,<sup>3</sup>  $1/N$  expansions in the Schwinger-boson representation,<sup>4</sup> modified spin-wave treatments,<sup>5,6</sup> and Green's-function random-phase-approximation (RPA) calculations.<sup>7</sup> It should be remarked, however, that although the spin fluctuations of the layered antiferromagnetic systems have predominantly two-dimensional behavior,<sup>1</sup> the interplane coupling  $J_{\perp}$ , albeit small, is responsible for driving the three-dimensional magnetic phase transition at a large Néel temperature.

In a previous paper<sup>8</sup> (henceforth referred to as paper I)

we have discussed the properties of the antiferromagnetic phase of these layered systems in the temperature range  $0 \leq T \leq T_N$  by retaining their full three-dimensional character (with  $J_{\perp} \neq 0$  and  $0 \leq \epsilon \leq 1$ ). To this end, we have relied on free-spin-wave (FSWA), random-phase (RPA), and modified random-phase (MRPA) treatments. We have shown therein that estimates of the anisotropy ratio  $\epsilon$  depend strongly on the theoretical approximation underlying the interpretation of the experimental results. We have also found that the first-nearest-neighbor instantaneous spin correlator increases with temperature and reaches a finite value at  $T_N$ . This correlator is to be interpreted as a short-range-order parameter, to be contrasted with the sublattice magnetization that characterizes the full long-range order. Our finding that finite-range correlations are strong at high temperature ( $T \approx T_N$ ) is actually consistent with the experimental evidence mentioned above.<sup>1,2</sup>

In this paper we extend the theoretical treatments of paper I to the high-temperature regime ( $T \geq T_N$ ) while keeping the anisotropy ratio  $\epsilon$  finite. We thus work with the RPA and MRPA decouplings within the Green's-function methods, thereby encompassing the approach of Ref. 7 which was limited to the RPA with  $\epsilon=0$ .

In paper I, we have emphasized that the persistence of intraplane spin correlations for  $T \approx T_N$  is favored by the quasi-two-dimensional character of the system. Similarly, we shall show in the following that the values  $\epsilon \sim 10^{-4}-10^{-5}$  reported for  $\text{La}_2\text{CuO}_4$  (Ref. 1) are compatible with a large value of the correlation length  $\xi_c$  up to temperatures well above  $T_N$ . We shall also show that the values of  $\xi_c$  obtained for  $T > T_N$  within the RPA and MRPA compare extremely well with the experimental inelastic-neutron-scattering data on  $\text{La}_2\text{CuO}_4$  (Ref. 1). In addition, our results suggest that  $\epsilon$  might vary with  $T$  by

1 or 2 orders of magnitude (depending on the theoretical approximation used to evaluate  $\xi_c$ ) in the temperature range covered by the neutron experiments. Our suggestion of a softening of  $\epsilon$  with temperature is also consistent with the reported pressure dependence of  $J_{\parallel}$  and  $T_N$ ,<sup>9,10</sup> where  $\epsilon$  appears to vary by almost 2 orders of magnitude from atmospheric pressure to 60 kbar.

The plan of the paper is the following. In Sec. II, we briefly recall the RPA and MRPA decouplings within a Green's-function treatment of the spin correlators, and present the results of the calculation of the correlation length  $\xi_c$  for  $T > T_N$  and arbitrary anisotropy  $0 \leq \epsilon \leq 1$ . In Sec. III we analyze the pressure experiments, and discuss their consequences in the context of the present work. In Sec. IV, we eventually discuss our results in connection with other theoretical calculations and experimental findings.

## II. MODEL HAMILTONIAN AND METHOD OF CALCULATION

### A. RPA solution

The spin Hamiltonian we consider is the same as in paper I, namely, the anisotropic nearest-neighbor Heisenberg model for spin- $\frac{1}{2}$  operators  $\vec{S}_i$  at site  $i$ :

$$H = J_{\parallel} \sum_{i, \Delta_{\parallel}} \vec{S}_i \cdot \vec{S}_{i+\Delta_{\parallel}} + J_{\perp} \sum_{i, \Delta_{\perp}} \vec{S}_i \cdot \vec{S}_{i+\Delta_{\perp}}, \quad (2.1)$$

where  $\Delta_{\parallel}$  and  $\Delta_{\perp}$  are the lattice constants in the basal plane and along the tetragonal symmetry axis, respectively.

Since we want to describe spin correlations above  $T_N$  where there is no long-range order, we follow Ref. 7 and add to  $H$  the interaction of the spin system with a fictitious external staggered magnetic field:

$$\delta H = - \sum_i h_i^{\dagger} S_i^z \quad (2.2)$$

with  $h_i^{\dagger} = h^{\dagger} \exp[-i\mathbf{Q} \cdot \mathbf{R}_i]$ . The wave vector  $\mathbf{Q}$  has the property

$$\exp[-i\mathbf{Q} \cdot \mathbf{R}_i] = \begin{cases} 1 & \text{if } \mathbf{R}_i \text{ is in the up (A) sublattice,} \\ -1 & \text{if } \mathbf{R}_i \text{ is in the} \\ & \text{down (B) sublattice.} \end{cases}$$

The field  $h_i^{\dagger}$  then produces an antiferromagnetic ordering above  $T_N$ , which disappears as soon as  $h^{\dagger} \rightarrow 0$ , and with the average  $z$  component of spins  $\langle S_i^z \rangle$  pointing in the direction of  $h_i^{\dagger}$  at each site  $i$ .

As in paper I, we consider the dynamic transverse spin-correlation function

$$\chi_{ij}^{+-}(\tau) = \langle T_{\tau} [S_i^{\dagger}(\tau) S_j^{-}(0)] \rangle, \quad (2.3)$$

where  $\tau$  is the Matsubara imaginary time,  $T_{\tau}$  denotes the time-ordering operator, and  $\langle \dots \rangle$  stands for thermal average. Within the RPA, the equation of motion for the Fourier transform of  $\chi^{+-}$  [cf. Eq. (2.6) of paper I] is simply obtained from Eq. (2.9) of paper I by replacing

$$\omega_0 \rightarrow \bar{\omega}_0 = \omega_0 + h^{\dagger} \equiv (1 + \lambda)\omega_0, \quad (2.4)$$

where  $\omega_0 = 2\langle S_A^z \rangle J_{\parallel}(z_{\parallel} + \epsilon z_{\perp})$  and  $\lambda = h^{\dagger}/\omega_0$ . In these expressions,  $z_{\parallel}$  is the number of first-nearest-neighbor sites within each plane and  $z_{\perp}$  the number of first-nearest-neighbor sites on adjacent planes.

The self-consistency condition for  $\langle S_A^z \rangle$  is now given by

$$\langle S_A^z \rangle = \frac{1/2}{1 + 2\psi} \quad (2.5)$$

with

$$\psi = \frac{1}{N} \sum_{\mathbf{q}}' \left[ \frac{\bar{\omega}_0}{\bar{\Omega}(\mathbf{q})} \coth \left[ \frac{\beta}{2} \bar{\Omega}(\mathbf{q}) \right] - 1 \right], \quad (2.6)$$

$N$  being the number of atomic unit cells,  $\beta = (k_B T)^{-1}$ , and with the understanding that the primed sum extends over the antiferromagnetic Brillouin zone. In Eq. (2.6)

$$\bar{\Omega}^2(\mathbf{q}) = \bar{\omega}_0^2 - \omega_1(\mathbf{q})^2, \quad (2.7)$$

where  $\omega_1(\mathbf{q})$  is given by

$$\omega_1(\mathbf{q}) = 2\langle S_A^z \rangle J_{\parallel} [z_{\parallel} \gamma_{\parallel}(\mathbf{q}) + \epsilon z_{\perp} \gamma_{\perp}(\mathbf{q})] \quad (2.8)$$

with  $\gamma_{\parallel}(\mathbf{q})$  and  $\gamma_{\perp}(\mathbf{q})$  defined below. Notice that, for finite  $h^{\dagger}$ ,  $\bar{\Omega}(\mathbf{q})$  has a finite limit as  $\mathbf{q} \rightarrow 0$ .

We now consider the limit  $h^{\dagger} \rightarrow 0$ . In the ordered antiferromagnetic phase ( $T < T_N$ ),  $\langle S_A^z \rangle \neq 0$  and  $\lambda = 0$  when  $h^{\dagger} \rightarrow 0$ . In the paramagnetic phase ( $T > T_N$ ), on the other hand,  $\lambda$  tends to a finite limit as  $h^{\dagger} \rightarrow 0$ , since  $\langle S_A^z \rangle \rightarrow 0$  correspondingly. In this limit, we can approximate  $\coth x \sim 1/x$  in Eq. (2.6). The self-consistency condition (2.5) then becomes an equation for the parameter  $\lambda$  for given  $\epsilon$  and  $T$ :

$$\frac{2}{N} \sum_{\mathbf{q}}' \frac{1 + \lambda}{(1 + \lambda)^2 - \gamma_{\epsilon}(\mathbf{q})^2} = \frac{T_N^{(\text{MF})}}{T}, \quad (2.9)$$

with the notation

$$\begin{aligned} \gamma_{\epsilon}(\mathbf{q}) &= \frac{z_{\parallel} \gamma_{\parallel}(\mathbf{q}) + \epsilon z_{\perp} \gamma_{\perp}(\mathbf{q})}{z_{\parallel} + \epsilon z_{\perp}}, \\ \gamma_{\parallel}(\mathbf{q}) &= \frac{1}{z_{\parallel}} \sum_{\Delta_{\parallel}} e^{i\mathbf{q} \cdot \Delta_{\parallel}}, \\ \gamma_{\perp}(\mathbf{q}) &= \frac{1}{z_{\perp}} \sum_{\Delta_{\perp}} e^{i\mathbf{q} \cdot \Delta_{\perp}}, \end{aligned} \quad (2.10)$$

and where  $k_B T_N^{(\text{MF})} = J_{\parallel}(z_{\parallel} + \epsilon z_{\perp})/2$  is the critical temperature at the mean-field level. The above equations extend those obtained in Ref. 7 for the isotropic two-dimensional antiferromagnet. Notice that for  $\lambda \rightarrow 0$ , Eq. (2.9) determines the critical temperature  $T_N^{(\text{RPA})}$  within the RPA. Notice also that, for a given  $\epsilon$ ,  $\lambda$  grows monotonically with  $T$  for  $T \geq T_N$ , and is asymptotically linear in  $T$  as  $T \rightarrow \infty$ .

### B. Calculation of $\xi_c(\epsilon, T)$ in RPA

We consider now the asymptotic form of the instantaneous spin correlator, which can be obtained from the correlation function  $\chi^{+-}$ . In the paramagnetic phase, one obtains, in the limit  $h^\dagger \rightarrow 0$ ,

$$\langle S_i^+ S_j^- \rangle = e^{-i\mathbf{Q}\cdot\mathbf{R}_j} \frac{T}{T_N^{(\text{MF})}} \frac{1+\lambda}{N} \sum_{\mathbf{q}}' \frac{e^{i\mathbf{q}\cdot(\mathbf{R}_i - \mathbf{R}_j)}}{(1+\lambda)^2 - \gamma_\epsilon(\mathbf{q})^2}. \quad (2.11)$$

The dominant contribution to Eq. (2.11) for  $|\mathbf{R}_i - \mathbf{R}_j| \rightarrow \infty$  comes from the neighborhood of  $\mathbf{q}=0$ , so we can write

$$\langle S_i^+ S_j^- \rangle e^{i\mathbf{Q}\cdot\mathbf{R}_j} \frac{T_N^{(\text{MF})}}{T} \cong \frac{\Delta_{\parallel}^2 \Delta_{\perp} (1+\lambda)}{\pi^2} \int_0^{\Lambda_{\parallel}} q_{\parallel} J_0(q_{\parallel} R_{\parallel}) dq_{\parallel} \int_0^{\Lambda_{\perp}} \left[ (1+\lambda)^2 - 1 + \frac{A}{2} q_{\parallel}^2 \Delta_{\parallel}^2 + B q_{\perp}^2 \Delta_{\perp}^2 \right]^{-1} dq_{\perp}, \quad (2.12)$$

where  $J_0(z)$  is the Bessel function of zero order,  $\Lambda_{\parallel}$  and  $\Lambda_{\perp}$  are cutoff parameters,  $R_{\parallel} = |\mathbf{R}_i - \mathbf{R}_j|$  for  $i$  and  $j$  belonging to the same basal plane, and where we have set  $A = z_{\parallel}/(z_{\parallel} + \epsilon z_{\perp})$  and  $B = \epsilon z_{\perp}/(z_{\parallel} + \epsilon z_{\perp})$ . Introducing at this point new integration variables  $\xi = \sqrt{A}/2q_{\parallel}\Delta_{\parallel}$  and  $\zeta = \sqrt{B}q_{\perp}\Delta_{\perp}$ , Eq. (2.12) becomes

$$\langle S_i^+ S_j^- \rangle e^{i\mathbf{Q}\cdot\mathbf{R}_j} \frac{T_N^{(\text{MF})}}{T} \cong \frac{2(1+\lambda)}{\pi^2} \frac{1}{A\sqrt{B}} \int_0^{\Lambda'_{\parallel}} \frac{\xi J_0(\sqrt{2/A}\xi R_{\parallel}/\Delta_{\parallel})}{\sqrt{(1+\lambda)^2 - 1 + \xi^2}} \tan^{-1} \left[ \frac{\sqrt{B}\Delta_{\perp}\Lambda_{\perp}}{\sqrt{(1+\lambda)^2 - 1 + \xi^2}} \right] d\xi. \quad (2.13)$$

In the two extreme cases where the argument of  $\tan^{-1}$  is either (a) very large or (b) very small, one gets

$$\langle S_i^+ S_j^- \rangle e^{i\mathbf{Q}\cdot\mathbf{R}_j} \frac{T_N^{(\text{MF})}}{T} \cong \frac{2(1+\lambda)}{\pi^2} \frac{1}{A\sqrt{B}} \begin{cases} \frac{\pi}{2} \left[ \frac{A}{2} \right]^{1/2} \frac{\Delta_{\parallel}}{R_{\parallel}} e^{-R_{\parallel}/\xi_c} & \text{(a)}, \\ \sqrt{B}\Delta_{\perp}\Lambda_{\perp} K_0(R_{\parallel}/\xi_c) & \text{(b)}, \end{cases} \quad (2.14)$$

where in both cases

$$\frac{\xi_c}{\Delta_{\parallel}} \equiv \left[ \frac{A}{2} \right]^{1/2} \frac{1}{\sqrt{(1+\lambda)^2 - 1}} \quad (2.15)$$

and  $K_0(z)$  is the modified Bessel function of order 0 that for large  $z$  behaves as

$$K_0(z) \sim \sqrt{\pi/2z} e^{-z}.$$

One thus obtains the *same* exponential decay of the spin correlator in both limits (a) and (b), and may therefore identify  $\xi_c$  given by Eq. (2.15) as the *correlation length* for all values of  $T$  and  $\epsilon$ . Notice that case (b) corresponds to the two-dimensional limit since  $B$  vanishes in that limit. The resulting correlation length then coincides with that found in Ref. 7 for the strictly two-dimensional case.<sup>11</sup>

### C. Calculation of $\xi_c(\epsilon, T)$ in MRPA

According to paper I, the MRPA replaces the (spin- $\frac{1}{2}$ ) operator  $S_i^z$  by its alternative expression [cf. Eq. (2.25) of paper I],

$$S_i^z = \left[ \frac{1-\alpha}{2} \right] (-\frac{1}{2} + S_i^+ S_i^-) + \left[ \frac{1+\alpha}{2} \right] (\frac{1}{2} - S_i^- S_i^+), \quad (2.16)$$

and takes for the parameter  $\alpha$  the value  $\alpha = 2\langle S_i^z \rangle$ . The resulting approximation entails the coupling of longitudinal to transverse fluctuations. MRPA further decouples higher-order correlators which involve four spin operators and which result from the replacement (2.16). The

MPRA decoupling thus has the effect of relating in a self-consistent way the long-range-order parameter  $\langle S_i^z \rangle$  to the short-range instantaneous correlator  $\langle S_{i+\Delta}^+ S_i^- \rangle$  (where in the anisotropic case  $\Delta$  can be either  $\Delta_{\parallel}$  or  $\Delta_{\perp}$ ). As in paper I we denote

$$\langle S_{i+\Delta}^+ S_i^- \rangle = \begin{cases} F_{\parallel} & \text{for } \Delta = \Delta_{\parallel}, \\ F_{\perp} & \text{for } \Delta = \Delta_{\perp}. \end{cases} \quad (2.17)$$

In the paramagnetic phase ( $T > T_N$ ), we can follow the same procedure used above for the RPA and introduce a staggered external field  $h_i^\dagger$ . In place of Eq. (2.6) we now obtain

$$\tilde{\psi} = \frac{1}{N} \sum_{\mathbf{q}}' \left[ \frac{(1+\tilde{\lambda})\tilde{\omega}(0)}{\tilde{\Omega}(\mathbf{q})} \coth \left[ \frac{\beta}{2} \tilde{\Omega}(\mathbf{q}) \right] - 1 \right], \quad (2.18)$$

where

$$\tilde{\omega}(\mathbf{q}) = 2\langle S_A^z \rangle \tilde{J}(\mathbf{q}), \quad (2.19a)$$

$$\tilde{J}(\mathbf{q}) = J_{\parallel} z_{\parallel} \gamma_{\parallel}(\mathbf{q})(1+2|F_{\parallel}|) + J_{\perp} z_{\perp} \gamma_{\perp}(\mathbf{q})(1+2|F_{\perp}|), \quad (2.19b)$$

$$\tilde{\Omega}(\mathbf{q}) = \sqrt{(1+\tilde{\lambda})^2 \tilde{\omega}(0)^2 - \tilde{\omega}(\mathbf{q})^2}, \quad (2.19c)$$

while the correlators  $F_{\parallel}$  and  $F_{\perp}$  are given by

$$F_{\parallel, \perp} = -2\langle S_A^z \rangle \frac{1}{N} \sum_{\mathbf{q}}' \gamma_{\parallel, \perp}(\mathbf{q}) \frac{\tilde{\omega}(\mathbf{q})}{\tilde{\Omega}(\mathbf{q})} \coth \left[ \frac{\beta}{2} \tilde{\Omega}(\mathbf{q}) \right]. \quad (2.20)$$

Equations (2.18)–(2.20), which define the MRPA decou-

pling for  $T \geq T_N$ , are identical to those introduced in paper I for  $T \leq T_N$  but for the replacement  $\tilde{\omega}(0) \rightarrow (1 + \tilde{\lambda})\tilde{\omega}(0)$ , where  $\tilde{\lambda} = h^\dagger / \tilde{\omega}(0)$ . In the paramagnetic phase  $\langle S_A^z \rangle$  vanishes when  $h^\dagger \rightarrow 0$  while  $\tilde{\lambda}$  remains finite in the limit.

The parameter  $\tilde{\lambda}$  can be self-consistently determined in the limit  $h^\dagger \rightarrow 0$  via the equation

$$\frac{2}{N} \sum_{\mathbf{q}} \frac{(1 + \tilde{\lambda})}{(1 + \tilde{\lambda})^2 - [\tilde{J}(\mathbf{q})/\tilde{J}(0)]^2} = \frac{\tilde{J}(0)}{2k_B T} \quad (2.21)$$

for given  $\epsilon$  and  $T$ . This equation generalizes to the MRPA Eq. (2.9) that holds for the RPA. In particular, for the two-dimensional case ( $\epsilon = 0$ ) Eq. (2.21) reduces to

$$\frac{2}{N} \sum_{\mathbf{q}} \frac{(1 + \tilde{\lambda})}{(1 + \tilde{\lambda})^2 - \gamma_{\parallel}(\mathbf{q})^2} = \frac{J_{\parallel} z_{\parallel} (1 + 2|F_{\parallel}|)}{2k_B T}, \quad (2.22)$$

which coincides with Eq. (39) of Ref. 7 when one sets  $F_{\parallel} = 0$  (and when a different definition of  $J_{\parallel}$  in the Hamiltonian is taken into account). Accordingly, for temperatures,  $T \ll T_{2D}^{(MF)} = J_{\parallel} z_{\parallel} / 2k_B$  (that correspond to  $\tilde{\lambda} \ll 1$ ) one gets a generalization of Eq. (29) of Ref. 7, in the form

$$\tilde{\lambda}_{2D} \cong 8 \exp \left\{ \frac{-\pi(1 + 2|F_{\parallel}|)T_{2D}^{(MF)}}{T} \right\}. \quad (2.23)$$

By the same token, the instantaneous spin correlator  $\langle S_i^+ S_j^- \rangle$  is given in the MRPA by a similar expression to Eq. (2.11) with  $T_N^{(MF)}$  replaced by  $\tilde{J}(0)/2k_B$  and  $\gamma_{\epsilon}(\mathbf{q})$  replaced by  $\tilde{J}(\mathbf{q})/\tilde{J}(0)$ . In particular, in the two-dimensional limit ( $\epsilon \ll 1$ ) we obtain the same relation between  $\xi_c / \Delta_{\parallel}$  and  $\tilde{\lambda}$  as that derived in the RPA from Eq. (2.15) for small  $\epsilon$  and  $\lambda$ , namely,

$$\frac{\xi_c}{\Delta_{\parallel}} \cong \frac{1}{2\sqrt{\tilde{\lambda}}}. \quad (2.24)$$

Combining Eqs. (2.23) and (2.24) yields the analytic result

$$\frac{\xi_c}{\Delta_{\parallel}} \cong \frac{1}{4\sqrt{2}} \exp \left\{ \frac{\pi(1 + 2|F_{\parallel}|)T_{2D}^{(MF)}}{2T} \right\} \quad (2.25)$$

in the two-dimensional limit, which implies that  $\xi_c$  gets enhanced in the MRPA with respect to the RPA by taking explicit account of the short-range spin correlations.

Previous calculations,<sup>3-6</sup> although based on different methods, have all arrived at the following form for the two-dimensional coherence length:

$$\xi_c^{(2D)}(T \rightarrow 0) = \frac{Bc}{k_B T} \exp \left\{ \frac{2\pi\rho_s}{k_B T} \right\}, \quad (2.26)$$

where  $B$  is a numerical coefficient,  $c$  the spin-wave velocity, and  $\rho_s$  the spin-stiffness constant. In particular, Eq. (2.26) has been obtained in Ref. 3 by including one-loop corrections within the nonlinear  $\sigma$  model. Inclusion of two-loop corrections in Ref. 3, however, leads to cancellation of the  $1/T$  prefactor:<sup>12</sup>

$$\xi_c^{(2D)}(T \rightarrow 0) = C \exp \left\{ \frac{2\pi\rho_s}{k_B T} \right\}. \quad (2.27)$$

Quantum Monte Carlo simulations confirm the result

(2.27),<sup>13</sup> and yield typically the values  $C/\Delta_{\parallel} \cong 0.27$  and  $\rho_s \cong 0.4J_{\parallel}$  which provide a good fit of the experimental data on  $\text{La}_2\text{CuO}_4$  (Ref. 1) via Eq. (2.27).

The RPA counterpart of Eq. (2.25) (i.e., with  $F_{\parallel} = 0$ ) yields instead the values 0.177 for the constant prefactor  $C/\Delta_{\parallel}$  and  $0.5J_{\parallel}$  for the spin-stiffness constant, respectively. This remarkable similarity between the RPA and more elaborate treatments in two dimensions ( $\epsilon = 0$ ) was already stressed in Ref. 7. As regards the MRPA result (2.25), on the other hand, there are no changes from the general form (2.27); the short-range-order correction in the exponential of Eq. (2.25), however, worsens the quantitative comparison with quantum Monte Carlo simulations since  $1 + 2|F_{\parallel}| \geq 1$ .

We shall anyhow postpone the comparison of the RPA and MRPA results for  $\xi_c$  with the data of Ref. 1 to Sec. IV, where numerical results will be presented for the more realistic case of a nonvanishing anisotropy ratio ( $\epsilon > 0$ ).

### III. PRESSURE DEPENDENCE OF THE ANISOTROPY RATIO $\epsilon$

Recent experiments have explored the pressure dependence of the antiferromagnetic properties of  $\text{La}_2\text{CuO}_4$  samples. We shall consider specifically two different sets of experiments,<sup>9,10</sup> in which the pressure dependence of  $J_{\parallel}$  and  $T_N$  was, respectively, measured. This will enable us to deduce the pressure dependence of  $J_{\perp}$ , assuming that  $\epsilon = 10^{-5}$  is a reasonable estimate of the anisotropy ratio at atmospheric pressure.

We begin by rewriting Eq. (2.22) of paper I, where the  $\epsilon$  dependence of  $T_N$  is approximately obtained in the analytic form

$$\frac{k_B T_N^{(RPA)}}{J_{\parallel}} = \frac{A}{B + \ln 1/\epsilon}, \quad (3.1)$$

$A$  and  $B$  being numerical constants. [Although expression (3.1) holds also within the MRPA, for the sake of definiteness we shall consider in this section only the RPA values for  $A$  and  $B$ .] We assume at this point that it is possible to account for the pressure dependence of the magnetic properties of  $\text{La}_2\text{CuO}_4$  with a Heisenberg model whereby the pressure acts only to modify  $J_{\parallel}$ ,  $\epsilon$ , and  $T_N$ . This implies that we consider Eq. (3.1) to hold at any given pressure by inserting the proper pressure-dependent values of  $J_{\parallel}(P)$ ,  $\epsilon(P)$ , and  $T_N(P)$ .

A simple manipulation of Eq. (3.1) yields then for the pressure dependence of  $\epsilon$

$$\ln \epsilon(P) = B \left[ 1 - \frac{e(P)}{t(P)} \right] + \frac{e(P)}{t(P)} \ln \epsilon(0), \quad (3.2)$$

where  $\epsilon(0)$  stands for the value of  $\epsilon$  at atmospheric pressure and with the notation

$$\begin{aligned} e(P) &= J_{\parallel}(P)/J_{\parallel}(0), \\ t(P) &= T_N(P)/T_N(0). \end{aligned} \quad (3.3)$$

The measured values of the ratios  $e(P)$  and  $t(P)$  have

been reported in Refs. 9 and 10, respectively, for  $\text{La}_2\text{CuO}_4$  samples. In particular,  $e(P)$  is found to follow approximately the linear trend

$$e(P) = 1 + 1.39 \times 10^{-3} P (\text{kbar}) \quad (3.4)$$

for  $P \lesssim 60$  kbar,<sup>9</sup> while  $t(P)$  follows the more marked linear trend

$$t(P) = 1 + 8.2 \times 10^{-3} P (\text{kbar}) \quad (3.5)$$

for  $P \lesssim 15$  kbar.<sup>10</sup> Thus, for  $P=15$  kbar we obtain  $e(P)/t(P) \cong 0.91$  and for  $P=60$  kbar we obtain  $e(P)/t(P) \cong 0.72$  (if we make the further reasonable assumption that the linear pressure dependence of  $T_N$  can be extrapolated up to 60 kbar). Equation (3.2) yields then the values  $3.7 \times 10^{-5}$  and  $5.8 \times 10^{-4}$  for  $\epsilon(P)$  at the two pressures, in the order. Notice that the variation of  $\epsilon(P)$  is *strongly nonlinear*, and that  $\epsilon$  turns out to vary by almost 2 orders of magnitude from atmospheric pressure to 60 kbar. From Eqs. (3.2) and (3.3) we can finally evaluate the ratio

$$\frac{J_{\perp}(P)}{J_{\perp}(0)} = e(P) \frac{\epsilon(P)}{\epsilon(0)}, \quad (3.6)$$

which takes the values 3.8 and 63 for  $P=15$  kbar and  $P=60$  kbar, respectively. This result would imply that  $J_{\perp}$  is extraordinarily sensitive to pressure, increasing by almost two orders of magnitude in 60 kbar.

This gigantic pressure effect on  $J_{\perp}$  was already noticed in Ref. 9, although by relying on a law for the dependence of  $T_N$  on  $\epsilon$  different from Eq. (3.1). It is worthwhile to comment briefly on this difference. According to Thio *et al.*,<sup>14</sup> the condition which determines  $T_N$  in terms of  $J_{\perp}$  is given by

$$J_{\perp} \chi_{2D}^{\dagger}(T_N) = 1, \quad (3.7)$$

where  $\chi_{2D}^{\dagger}(T)$  is the temperature-dependent two-dimensional staggered static susceptibility. Equation (3.7) has the meaning of an instability condition for the intraplane coupling of two-dimensional magnetic domains and depends crucially on the form one assumes for the function  $\chi_{2D}^{\dagger}(T)$ . Thio *et al.* approximate for  $T \ll T_N^{(\text{MF})}$  ( $= 2J_{\parallel}/k_B$  in the two-dimensional case)

$$\chi_{2D}^{\dagger}(T) \cong \frac{[\xi_{2D}(T)/\Delta_{\parallel}]^2}{k_B T}, \quad (3.8)$$

which reduces Eq. (3.7) to the form

$$J_{\perp} \left[ \frac{\xi_{2D}(T_N)}{\Delta_{\parallel}} \right]^2 \cong k_B T_N. \quad (3.9)$$

This is the dependence of  $T_N$  on  $\epsilon$  (apart from a coefficient of order unity) which was used in Ref. 9 to estimate the pressure effect on  $J_{\perp}$ .

It can be readily shown that the RPA result (3.1) can also be cast in the form (3.7) (again apart from numerical coefficients of order unity), but with the replacement of the RPA dependence of  $\chi_{2D}^{\dagger}$  on  $T$  when  $T \ll T_N^{(\text{MF})}$ , namely,

$$\chi_{2D}^{\dagger}(T) \cong \frac{[\xi_{2D}(T)/\Delta_{\parallel}]^2}{k_B T_N^{(\text{MF})}} \quad (3.10)$$

instead of Eq. (3.8). The RPA approach thus replaces the actual  $T_N$  on the right-hand side of Eq. (3.9) by its much larger mean-field value  $T_N^{(\text{MF})}$  (when  $\epsilon \ll 1$ ), with the net effect of somewhat reducing the pressure dependence of  $J_{\perp}$ .

The strong pressure dependence of the anisotropy ratio  $\epsilon$  discussed here for  $\text{La}_2\text{CuO}_4$ , although it may look rather surprising,<sup>9</sup> is indeed consistent with the marked temperature dependence of  $\epsilon$  which we shall discuss in the next section by comparing our calculation of  $\xi_c(\epsilon, T)$  with inelastic-neutron-scattering data on the same material.

#### IV. DISCUSSION OF THE NUMERICAL RESULTS AND CONCLUSIONS

We have shown in Sec. II how the correlation length  $\xi_c$  can be obtained within the RPA in terms of the parameter  $1+\lambda$  defined by the integral equation (2.9) [and within the MRPA in terms of the analogous parameter  $1+\tilde{\lambda}$  defined by Eq. (2.21)]. We have also remarked that, for given  $\epsilon$ ,  $1+\lambda \rightarrow 1$  at the critical temperature  $T_N$  while  $1+\lambda \cong T/T_N^{(\text{MF})}$  for  $T \gg T_N^{(\text{MF})}$ . [Recall that  $k_B T_N^{(\text{MF})} = DJ_{\parallel}$ , where  $D = (z_{\parallel} + \epsilon z_{\perp})/2$  can be regarded as an *effective dimensionality* of the system for  $0 < \epsilon < 1$ , which interpolates between three ( $\epsilon=1$  and  $D=3$ ) and two dimensions ( $\epsilon=0$  and  $D=2$ ).] In the paramagnetic phase we are considering in this paper,  $T_N$  and  $T_N^{(\text{MF})}$  act thus as the low- and the high-temperature scales, respectively.

Numerical results for the parameter  $1+\lambda$  given by Eq. (2.9) within the RPA are shown in Figs. 1–3 as a function

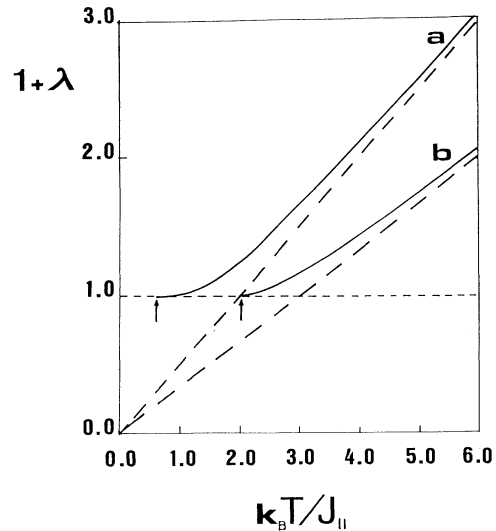


FIG. 1. The parameter  $1+\lambda$  calculated within the RPA vs  $k_B T/J_{\parallel}$  for (a)  $\epsilon=10^{-3}$  and (b)  $\epsilon=1$ . Dashed lines represent the respective asymptotes for  $T \gg T_N^{(\text{MF})}$  and arrows locate the Néel temperature  $T_N$  in the two cases.  $1+\lambda$  is defined by Eq. (2.9) of the text.

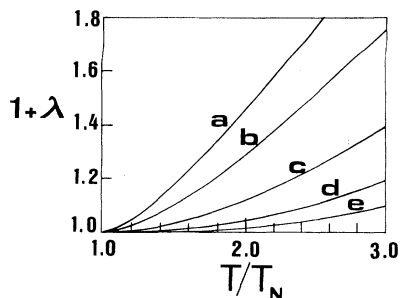


FIG. 2. The parameter  $1+\lambda$  calculated within the RPA vs  $T/T_N$  for (a)  $\epsilon=1$ , (b)  $\epsilon=10^{-1}$ , (c)  $\epsilon=10^{-2}$ , (d)  $\epsilon=10^{-3}$ , and (e)  $\epsilon=10^{-4}$ .

of  $T$  and  $\epsilon$  (similar results are obtained within the MRPA, but they are not reported). In particular, in Fig. 1 the parameter  $1+\lambda$  is plotted versus the reduced temperature  $k_B T/J_{\parallel}$  for two different values of  $\epsilon$ , showing that  $1+\lambda$  reaches its asymptotic value for large  $T$  only rather slowly. It is further instructive to plot  $1+\lambda$  versus the rescaled temperature  $T/T_N$ , which is possible in our case since  $T_N$  can be expressed in terms of  $J_{\parallel}$  and  $\epsilon$  only [cf. Eq. (3.1)]. Figure 2 shows that, at any given value of  $T/T_N$ ,  $\lambda$  can be made arbitrarily small by decreasing the value of  $\epsilon$ . According to Eq. (2.15), this result implies that  $\xi_c/\Delta_{\parallel}$  can be quite large even for temperatures well above  $T_N$  whenever  $\epsilon$  is sufficiently small (i.e., in the *quasi-two-dimensional* case). This is consistent with the experimental finding,<sup>1</sup> as discussed below in more detail. Finally, in Fig. 3 the parameter  $1+\lambda$  is plotted versus  $\epsilon$  for two characteristic temperatures. Notice that  $1+\lambda$  essentially saturates at its two-dimensional value when  $\epsilon \approx 10^{-3}$ , a value that thus characterizes the *crossover* from three to two dimensions for an anisotropic Heisenberg system also in the paramagnetic phase. We recall in

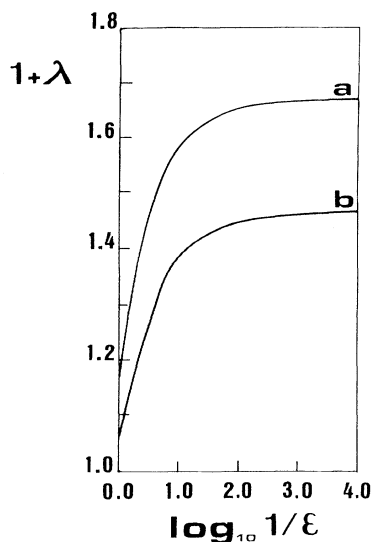


FIG. 3. The parameter  $1+\lambda$  calculated within the RPA vs  $\log_{10} 1/\epsilon$  for (a)  $k_B T/J_{\parallel}=3.0$  and (b)  $k_B T/J_{\parallel}=2.5$ .

this context that one of the main results of paper I was just that most properties of the anisotropic Heisenberg antiferromagnet saturate at  $\epsilon \approx 10^{-3}$  as  $\epsilon$  decreases from 1 to 0, the only exception to this rule being the Néel temperature which has to vanish in the limit  $\epsilon \rightarrow 0$ .

Once the parameter  $1+\lambda$  has been calculated, the correlation length  $\xi_c$  can be obtained from Eq. (2.15) within the RPA (and from a similar expression within the MRPA). Figures 4 and 5 show the RPA and MRPA results for  $\xi_c$ , in the order, versus the rescaled temperature  $T/T_N$  for three different values of  $\epsilon$  all verging on the two-dimensional side. The experimental results for  $\text{La}_2\text{CuO}_4$  from Ref. 1 are also shown for comparison, together with the strictly two-dimensional results versus the rescaled temperature  $T/T_N$  which is associated with the corresponding value of  $\epsilon$  [cf. Eq. (2.25) and the similar expression within the RPA]. Accordingly, the two-dimensional curves for different  $\epsilon$  are mutually displaced since the horizontal scale varies with  $\epsilon$ . In Figs. 4 and 5 the experimental results for  $\xi_c$  are plotted versus the rescaled temperature  $T/T_N^{\text{expt}}$  (for the particular sample reported  $T_N^{\text{expt}}=195$  K). Notice that fits to the experimental data obtained in Ref. 13 via Eq. (2.27) are *strictly two-dimensional*, that is for  $\epsilon=0$ , and require adjusting  $J_{\parallel}$  as a fitting parameter. In other words, looked at from the present approach, those fits require *two parameters*, namely,  $J_{\perp}$  and  $J_{\parallel}$ . Our results for  $\xi_c$  versus  $T/T_N$  contain instead *only one parameter*, namely,  $\epsilon$ , which has the advantage of being the (dimensionless) *ratio* of the two coupling constants of the model and of determining the universality class of the system. Notice further that, as  $T/T_N$  increases,  $\xi_c(\epsilon, T)$  converges to  $\xi_c^{\epsilon(2D)}(T)$  with a crossover temperature that depends on  $\epsilon$  and on the approximation.

From the comparison of our results with the experimental values of  $\xi_c/\Delta_{\parallel}$  shown in Figs. 4 and 5 we may conclude the following.

(i) There is reasonable agreement between the experimental values and our calculations *for a given value of  $\epsilon$*  (within both RPA and MRPA) if we assume that  $\epsilon \sim 10^{-4} - 10^{-6}$ .

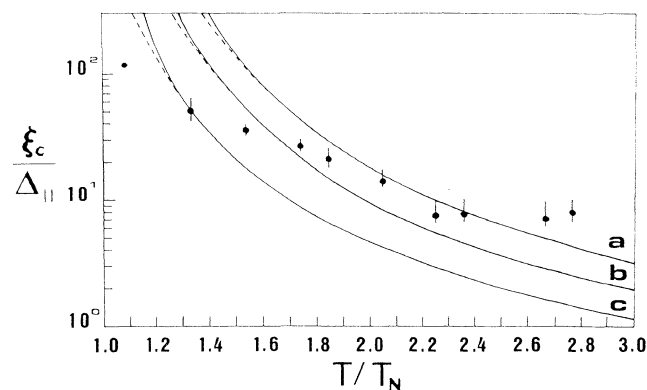


FIG. 4. Correlation length  $\xi_c$  in units of  $\Delta_{\parallel}$  calculated within the RPA vs  $T/T_N$  for (a)  $\epsilon=10^{-6}$ , (b)  $\epsilon=10^{-5}$ , and (c)  $\epsilon=10^{-4}$ . Dashed lines are the corresponding two-dimensional results as explained in the text.

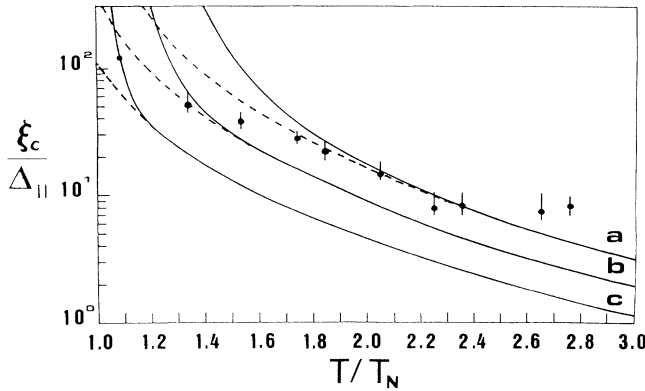


FIG. 5. Same as in Fig. 4 within the MRPA.

(ii) The agreement is best in an intermediate range of the rescaled temperature  $T/T_N$ , say for  $1.4 \lesssim T/T_N \lesssim 2.4$ .

(iii) For small values of  $T/T_N$  (or, equivalently, for large values of  $\xi_c/\Delta_{||}$ ) the theoretical values for  $\xi_c$  are larger than the experimental ones. This may be due to physical limitations affecting  $\xi_c$ , originating, for instance, from crystal grain boundaries or other defects.

(iv) For large values of  $T/T_N$  (or small  $\xi_c/\Delta_{||}$ ) we unavoidably expect discrepancies between our results and the experimental values of  $\xi_c$ , owing to the approximate method we have used in Sec. II to calculate the asymptotic behavior of the instantaneous spin correlator.

(v) A better agreement between our calculation and the experimental results is obtained if one assumes that, beginning at  $T/T_N \cong 1.4$ ,  $\epsilon$  starts decreasing with increasing  $T$  up to  $T/T_N \cong 2.4$  according to the MRPA. As already noted, the main physical difference between both approximations is a better treatment of the transverse and longitudinal fluctuations in the MRPA as compared to the RPA. Since, upon changing from RPA to MRPA the required variation of  $\epsilon$  decreases by 1 order of magnitude, one could perhaps assume that the exact theoretical calculation of  $\xi_c$  would yield a good fit with a fixed  $\epsilon$ . Our suspicion that this might not be the case is based upon the large variation of  $\epsilon$  with pressure which seems to be implied by experiments under hydrostatic pressure. It looks physically reasonable on this basis that this softening of  $\epsilon$  with increasing temperature is correlated with the hardening of  $\epsilon$  with increasing pressure discussed in Sec. III.

These conclusions call for a further analysis of the actual mechanism responsible for the interplane effective exchange coupling and of its dependence on thermodynamic variables like  $T$  and  $P$ .

We conclude this section by commenting on the relationship between the RPA and MRPA approaches through the temperature dependence of the first-nearest-neighbor instantaneous spin correlators  $F_{||}$  and  $F_{\perp}$ . It is expected that these approaches coincide when  $T/T_N$  is sufficiently large, owing to the decrease of  $|F_{||}|$  and  $|F_{\perp}|$  as  $T$  grows, which quenches the corrections to the RPA introduced by the MRPA. Figure 6 shows that indeed

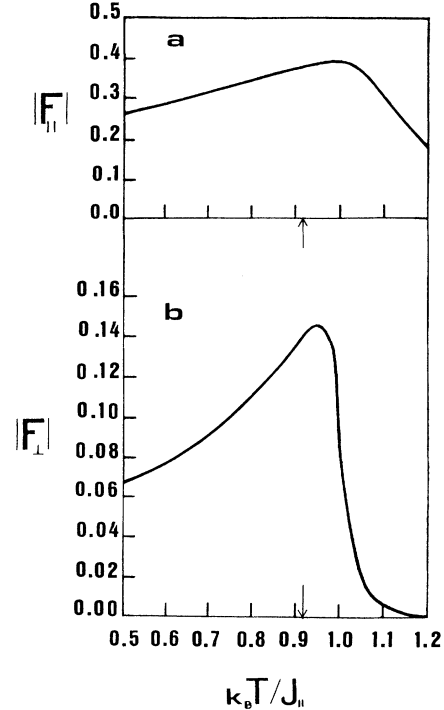


FIG. 6. First-nearest-neighbor instantaneous spin correlators within the MRPA vs  $k_B T/J_{||}$  for  $\epsilon=10^{-3}$ : (a)  $|F_{||}|$  and (b)  $|F_{\perp}|$  (the horizontal scale is the same for both curves). Arrows locate the value of  $T_N$ .

the interplane short-range-order parameter  $|F_{\perp}|$  drops abruptly as  $T$  increases above  $T_N$ , while the intraplane short-range-order parameter  $|F_{||}|$  decreases instead fairly slowly. This result indicates that the convergence of the MRPA to the RPA will actually be effective only at temperatures substantially larger than  $T_N$ , as it depends on the vanishing of both correlators  $F_{||}$  and  $F_{\perp}$ . The results shown in Fig. 6 are also quite interesting by themselves because they clearly demonstrate that *only intraplane spin correlations persist for  $T \gtrsim T_N$  when  $\epsilon \gtrsim 10^{-3}$* , thus favoring the persistence of two-dimensional localized excitations at high temperature. In this context, it is worth noticing the remarkable resemblance between the experimental data reported in Ref. 15 (and, specifically, the top part of Fig. 2 therein) with our Fig. 6(a) over the *whole* temperature range covered by our calculation (a resemblance that we have already noticed in paper I but for  $T \leq T_N$ ).

#### ACKNOWLEDGMENTS

N. M. and S. S. acknowledge support from Financiadora Nacional de Estudos e Projetos (FINEP) of Brasil. N. M. also acknowledges partial financial support from Conselho Nacional de Pesquisas Científicas e Tecnológicas (CNPq) of Brasil, from Consiglio Nazionale delle Ricerche (CNR) of Italy, and from Consorzio Interuniversitario Nazionale per la Fisica della Materia (INFN) of Italy.

- <sup>1</sup>Y. Endoh *et al.*, Phys. Rev. B **37**, 7443 (1988).  
<sup>2</sup>J. M. Tranquada *et al.*, Phys. Rev. B **38**, 2477 (1988).  
<sup>3</sup>S. Chakravarty, B. I. Halperin, and D. Nelson, Phys. Rev. B **39**, 2344 (1989).  
<sup>4</sup>D. Arovas and A. Auerbach, Phys. Rev. B **38**, 316 (1988).  
<sup>5</sup>M. Takahashi, Phys. Rev. B **40**, 2494 (1989).  
<sup>6</sup>J. E. Hirsch and S. Tang, Phys. Rev. B **40**, 4769 (1989).  
<sup>7</sup>D. A. Yablonskiy, Phys. Rev. B **44**, 4467 (1991).  
<sup>8</sup>N. Majlis, S. Selzer, and G. C. Strinati, Phys. Rev. B **45**, 7872 (1992).  
<sup>9</sup>M. C. Aronson *et al.*, Phys. Rev. B **44**, 4657 (1991).  
<sup>10</sup>S. Katano *et al.*, J. Phys. Soc. Jpn. **58**, 3890 (1989).  
<sup>11</sup>An alternative definition of the correlation length  $\xi_c$  [cf. A. Singh and Z. Tešanović, Phys. Rev. B **45**, 7258 (1992)] introduces  $\xi_c$  as the inverse momentum infrared cutoff needed to make the staggered moment to vanish at the given temperature in the paramagnetic phase.  
<sup>12</sup>A similar result was also obtained in Ref. 11.  
<sup>13</sup>E. Manousakis, Rev. Mod. Phys. **63**, 1 (1991).  
<sup>14</sup>T. Thio *et al.*, Phys. Rev. B **38**, 905 (1988).  
<sup>15</sup>G. Shirane *et al.*, Phys. Rev. Lett. **59**, 1613 (1987).